



Research Article

CRYSTAL ENGINEERING OF SALBUTAMOL SULPHATE PRODUCED BY *IN-SITU* MICRONIZATION TECHNIQUE FOR DRY POWDER INHALATION (DPI) TO IMPROVE THERAPEUTIC EFFICIENCY: OPTIMIZATION OF PROCESS PARAMETERS

P. S. Uttekar*, P. D. Chaudhari

Institute of Pharmacy, National Institute of Medical Sciences (NIMS) University, Shobhanagar, Jaipur, India

*Corresponding Author: Email pravinsuttekar@yahoo.co.in

(Received: May 14, 2012; Accepted: July 19, 2012)

ABSTRACT

The purpose of this study was to produce of microparticles for Dry Powder Inhalation, produced by environmentally driven *In-situ* Microcristonization technique at different processing parameters, for inhalation therapy. Typically particle size reduction process employs jet-milling technology which can be destructive to the solid-state properties of the particles. Salbutamol Sulphate, as one of the β_2 -adrenoceptor stimulant commonly used in the treatment of bronchial asthma by pulmonary delivery. The objective of the current work was to developed microcrystals by using *In-situ* Microcristonization technique with different processing parameters. A response surface type central composite design were employed using Design-Expert 5.0 software (Stat Ease, QD Consulting, Penzance, UK) with the factors investigated were stirrer speeds investigated were 500(-1), 1000(0) and 1500 (1) rpm, addition rate of non-solvent i.e ethanol was studied at 50(-1), 100(0) and 150(1) g /min and stabilizer conc. were 0.5(-1), 1(0) and 1.5 % (1). In the bottom up technique of micro sizing we use *in-situ* micronization technique which carried out using the solvent change method in presence of HPMC as stabilizing agent. The suspension was spray dried thereafter. Optimize the process variables for less mean particle size and high Fine Particle Fraction (FPF). Spray dried crystals were subjected to XRD, FTIR, DSC and SEM analysis for stability. The PSD and FPF also depended on the balance of meso and micromixing determined by the crystallization conditions. Optimized formulation was identified and characterized to determine their suitability for pulmonary delivery by using MSLI. Optimized formulation showed the highest FPF loaded and FPF emitted of 78 (1%) and 84 (3%) respectively, depositing mainly on stages 3 and 4, with much lower amounts collected on the higher stages of the MSLI.

Keywords: Salbutamol sulphate, *In-situ* micronization technique, Central Composite Design, Crystal engineering.

INTRODUCTION

Inhalation route of administration was presents as an ideal route to deliver active pharmaceutical ingredients (APIs) to the body in order to manage a wide range of local (i.e. asthma) and systemic (i.e. diabetes) disease states with improved pharmacokinetic properties.¹⁻³ The pulmonary system comprises of two main sections, namely the upper and lower respiratory tracts. Upper respiratory track associate with cilia/mucus as that of lower respiratory track associated nonciliated and bathed in pulmonary surfactant.⁴

Drug delivery to the body via the respiratory route is far from simple and as a result significant interest has arisen in

producing advanced inhaled formulations (i.e. nanoparticles; modified release particles, and highly porous microparticles) to maximize both deposition and interaction profiles with internal lung surfaces to ultimately improve therapeutic outcomes.⁵⁻¹¹ In the past Global Initiative for Chronic Obstructive Lung Disease guidelines,' it is concluded that acute exacerbations of chronic obstructive pulmonary disease (COPD) be treat with increased or more frequent doses or both of the patient's existing bronchodilator therapy.¹² In addition, for patients using Salbutamol, which is the gold standard bronchodilator agent in this pathologic

condition and induces a fast (within 2 to 3 minutes) bronchodilation, an acute exacerbation of COPD may require higher than customary doses.¹³

There are three ways or dosage forms to achieve Pulmonary delivery of active compounds i.e Metered Dose Inhalers (MDIS), Dry Powder Inhalers (DPIS) And Nebulizers. Nature of propellant and state of drug differentiate these dosage forms from each other. Particle size and their distribution governs the availability of drug to the lower respiratory region for the absorption and show system or local action. It is generally agreed that this particle size is in the range of 1–5 μm for “classical” drug particles. In the case of engineered particles having a low density, e.g. porous particles, the true particle size might be larger.^{14, 15}

Traditional techniques such as jet – milling for the particle size reduction have major limitation due to their effect on powder product characteristics such as size, shape, morphology, surface properties, and electrostatic charge.¹⁶

In addition, the jet-milled powders exhibit a broad particle size distribution and lower Fine Particle Fraction(FPF).¹⁷ Surfaces in mechanically micronized powders are not naturally grown as the crystal cleaves at the crystal face with the smallest attachment energy.¹⁸ Milling processes was several disadvantages such as decrease of crystallinity and chemical degradation of API because of their higher energy inputs.¹⁹⁻²⁰

As a thermodynamically-activated surface is created, the surface properties and thus the drug substance properties are altered.²¹⁻²² The conversion of crystalline solid surfaces into partially amorphous solid surfaces leads to a “dynamic nature” of the micronized drug.²³⁻²⁴ Thus, disordered structures in the material influence the performance in formulations and processing properties such as powder flow, as micronized powders with a higher energetic surface show poorer flow properties.²⁵⁻²⁶

As mechanically micronized powders show high particulate cohesion forces, the drug may be less effectively delivered from a DPI after size reduction than larger particles as shown for micronized (median size = 1.6 μm) and milled (7.2 μm) nedocromil sodium.²⁷

Crystal engineering in the context of this research article is taken as the design of molecular solids in the broadest sense with the aim of modifying specific physical or chemical

properties. In this study we explain diverse aspects of crystal engineering which may be used to manipulate the solubility, dissolution rate and micromeritic properties of the parent molecular components in the crystalline state. At the centre of these available approaches is the need to change surface and molecular assembly in equilibrium with a solution. This study also introduces aspects of the fundamental concepts of crystallization and describes the principles of crystal engineering which are typically used to control crystal size, shape and crystalline form. Although the primary focus considers the crystalline state, some reference will also be made to the utility of amorphous materials, with a brief summary of their use in enhancing drug dissolution and bioavailability.²⁸

In the present study, we applied controlled crystallization technique to produce Salbutamol sulfate, a β 2-adrenoceptor stimulant commonly used in the treatment of bronchial asthma. It has been found that spraydrying aqueous solution of Salbutamol sulphate will lead to an amorphous powder. In contrast, if the antisolvent precipitate in the suspension collected in presence of stabilizer is crystalline, then the resulting powder produced from spray drying of the suspension would be crystalline. In this paper a new approach combining *in-situ* micronization and spray drying to prepare fine powders suitable for inhalation is reported, along with the solid-state properties and aerosol performance of the powders.

2. Materials and Methods

2.1. Materials.

Salbutamol sulphate was supplied from Cipla Pharmaceuticals, Mumbai, Maharashtra, India. HPMC were purchased from Colorcon India Limited, Mumbai, Maharashtra, India. Ethanol (A.R. grade) was purchased from Loba Chemie Pvt. Ltd, Mumbai, India.

2.2. In- situ Micronization

2.2.1. Crystallization Procedure

In the bottom up technique of micro sizing we use *in-situ* micronization technique which carried out using the solvent change method in presence of HPMC as stabilizing agent. The process was carried out at room temperature. In the first step the 20 ml of saturated drug solution was dissolved in 100 ml of water under varying concentration of HPMC (0.5 to 1.5%). As non-solvent, which is miscible with water, ethanol

was used. Solvent to non-solvent ratio were kept constant i.e 1:8. The non-solvent i.e. ethanol was poured at a controlled rate using a model 505S peristaltic pump (Watson Marlow Bredel Pumps Ltd., Falmouth, UK) under stirring conditions using a magnetic stirrer. By batch-wise mixing of the two liquids (1:8) dispersion is formed as the drug is precipitated.

29

2.2.2. Spray Drying of Powder

After spray-drying (Mini Spray dryer, LU 22, Labultima, Mumbai, India) the prepared dispersion under standardized conditions: inlet temperature, 120 °C; outlet temperature, 80 °C; aspirator flow rate, 45 Nm³/h; 0.5mm nozzle; feed pump flow rate, 3 ml/min; cycle time, 120 min, resulting in a free-flowing, micron-sized drug powder. In this study, spray-drying was not used to form particles as if solutions were to be dried, but to dry the pre-formed particles. As the drug powder micronized using this technique is prepared directly in the micron-sized state during the particle formation without any further size reduction, this technique can be described as 'In-situ-micronization'.

2.2.3 Experimental design for the optimization of crystallization conditions

A response surface type central composite design were employed using Design-Expert 5.0 software (StatEase, QD Consulting, Penzance, UK) with linear as design model. The factors investigated were agitation rate, stabilizer conc. and addition rate. The stirrer speeds investigated were 500(-1), 1000(0) and 1500 (1) rpm, addition rate of non-solvent i.e. ethanol was studied at 50(-1), 100(0) and 150(1) g /min and stabilizer conc. were 0.5(-1), 1(0) and 1.5 %(1).

2.3. Solid-State Characterization.

2.3.1. X-ray diffraction studies

Powder X-ray patterns were recorded for pure drug and spray dried product using a Bruker AXS diffractometer (Bruker AXS GmbH, Germany) with a PSD-50M detector and EVA Application Software version 6. Measurements were performed with a Cu Ka radiation source at 40 kV voltage, 30 mA current and a maximum scanning speed of 2°/min.

2.3.2. Differential scanning calorimetry

DSC curves were obtained for pure drug and spray dried product by a Differential Scanning Calorimeter (DSC 821e, Mettler-Toledo, Switzerland) at a heating rate of 5 K/min from 0 to 340°C under nitrogen.

2.3.3. Scanning Electron Microscopy

Particle morphology was examined by Scanning Electron Microscopy (SEM) (S250MK, Cambridge, U.K.) operating at 19 keV or SEM (JSM-6360LV, JEOL, Japan) operating at 20 keV. The pure drug and spray dried powder could be characterized as dry powder. Samples were mounted on the copper stub by copper tape and sputter coated with Au at 6 mA for 3 min using a sputter coater (KYKY SBC-12, Beijing, China) under an Ar atmosphere.

2.3.4 Fourier transform infrared (FT-IR) spectroscopy

FT-IR were taken by FT-IR instrument (Perkin Elmer, USA) for different Salbutamol sulphate samples at scanning range between 450 cm⁻¹ and 4000 cm⁻¹. Each sample (several milligrams) was placed in the middle of the sample stage and a force applied (50 bar) using the top of the arm of the sample stage. After obtaining sharp peaks of appropriate intensity, the spectra acquired were the results of averaging four scans at 1 cm⁻¹.

2.3.5 Powder flow characterisation

Carr's index (CI) and angle of repose (α) were measured for spray dried Salbutamol sulphate powders as an indication of powder flowability. Each powder was filled into a 5 mL measuring cylinder and after recording the volume (bulk volume) the cylinder was tapped 100 times under ambient conditions (20 °C, 50% RH) and the new volume (tap volume) was recorded. It has been observed that 100 taps was sufficient to attain the minimum volume of the spray dried Salbutamol sulphate powders bed. Then, bulk density (Db), tap density (Dt), Carr's Index (CI), and porosity for each spray dried Salbutamol sulphate powders were calculated. The powders were subjected to bulk density and tapped density determination using Tapped density tester USP II (Veego, India). Angle of repose was measured by the method adapted from (Kaialy et al., 2011a). In brief, a pile was built by dropping 1 g of each through a 75 mm flask on a flat surface. Angle of repose (α) was calculated using the following equation 1 (where h is the height of the powder cone, and D the diameter of the base of the formed powder pile).

$$\tan \alpha = 2h/D \dots \dots \dots (1)$$

2.3.6 Particle size and distribution determination

Particle sizing was carried out by laser diffraction using the Malvern MastersizerX (Malvern Instruments Ltd., Malvern, UK) equipped with a 100 mm focal length lens and an MS7 magnetically stirred cell using the 2 NHE software presentation. The sizing methods were validated according to ISO 13320 (1990) standards. The spray dried Salbutamol sulphate powders (approximately 1 mg) were added to an 8 mL glass vial and 2 mL of filtered dispersant was added. The suspension was sonicated (BMI 599, Biomedica) in a water bath for 5 min to allow dispersion of the particles and aliquots were added successively to the sample cell by means of a Gilson pipette to achieve a satisfactory obscuration level (20% obscuration) and allowed to equilibrate for 60 s. Mean Particle size and Particle size distribution measurements were taken with each batch.

2.3.7. Aerodynamic particle size analysis

The dispersion behaviour of the spray dried Salbutamol sulphate powders were assessed using an Aerolizer (Novartis Pharmaceutical, Australia) as the inhaler coupled through a USP stainless steel throat to a Multistage Liquid Impinger (MSLI, Copley, U.K.), operating at 60 L/min controlled by the flow meter (DMF2000, Copley, U.K.) for 4 s. The MSLI is a versatile five-stage cascade impactor which can be used for determining the Dae distribution of Dry Powder Inhalation (DPI). The design is such that at a flow rate of 60 L/min, the cut off diameters of stages 1, 2, 3, and 4 are 13, 6.8, 3.1, and 1.7 μm , respectively. Stage 5 comprises an integral paper filter to capture the remaining fraction of particles less than 1.7 μm . By evaluating the DPI, it is then possible to calculate the mass fraction of drug particles smaller than 5 μm in the aerosol cloud, i.e., fine particle fraction (FPF). For MSLI, the FPF loaded and FPF emitted are defined as follows:

$$\text{FPF loaded} = \frac{\text{powder mass on stage 3 + stage 4 + filter}}{\text{total mass recovered}} \quad (2)$$

$$\text{FPF emitted} = \frac{\text{powder mass on stage 3 + stage 4 + filter}}{\text{total mass recovered} - \text{capsule and device retention}} \quad (3)$$

where the capsule and device retention is the mass of drug remaining in the capsules and the device. Stages 1-4 of MSLI were injected into 20.0 mL of methanol via a 0-5000 μL pipet (Transforpette, Brand, Germany), and the filter stage of MSLI is covered with a GF/A filter paper (70mm, Whatman, U.K.). The powder (10.00 (0.50 mg) was filled into Vcaps capsules (size 3, Capsuge, Suzhou, China). After analysis, the capsule, inhaler, throat, and filter paper were carefully rinsed with 20 mL of methanol. The MSLI itself was tightly sealed with Parafilm (Pechiney Plastic Packaging, USA) to avoid evaporation losses and gently shaken for 5-10 min to dissolve drug from each stage. Each experiment was performed in duplicate. Salbutamol sulphate deposited at different locations was assayed by U. V Spectrophotometry.³⁰

3. Results and Discussion

3.1 Physico-chemical characterization

3.1.1 X-ray diffraction studies

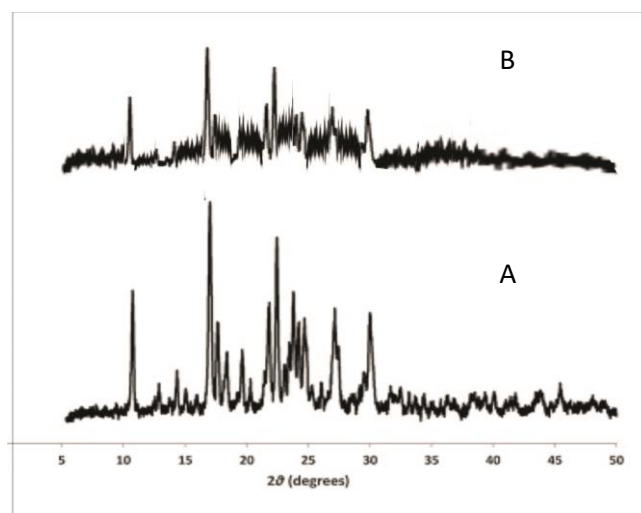


Figure 1. X-ray diffraction patterns of various Salbutamol sulphate dry powders: (A) commercial Salbutamol sulphate product; (B) Spray dried product.

X-ray diffraction (figure 1) is the potential tool for evaluation of stability during storage and use. Crystalline nature is preferable because of their thermodynamic stability than the amorphous nature. The PXRD patterns of in-situ-micronized Salbutamol sulphate show sharp peaks attributed to its crystalline nature but high baseline noise and the peaks with smaller heights were the two differences observed in comparison with pure Salbutamol sulphate after

storage at $40 \pm 8^\circ\text{C}/75\%$ relative humidity for 3 months. High baseline noise was due to coverage with amorphous HPMC and peaks with a smaller height were attributed to crystal size and crystallinity. Therefore, the peak heights of the microcrystals were expected to be slightly smaller than that of the standard crystalline powder.

3.1.2 Differential scanning calorimetry

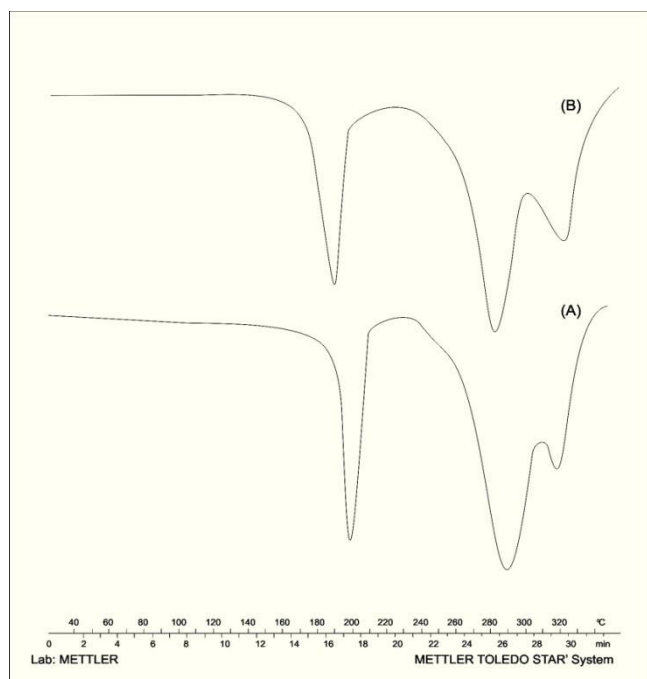


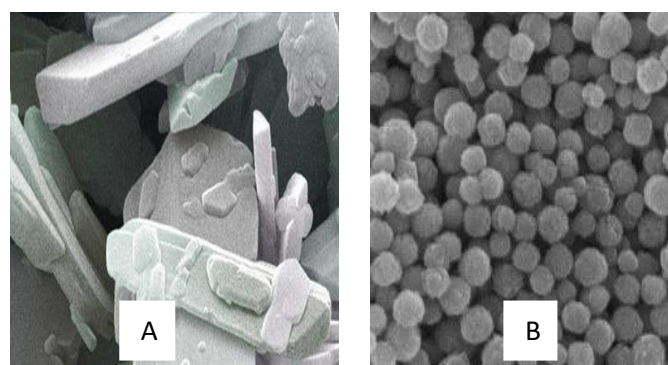
Figure 2. The DSC thermograms of Salbutamol sulphate pure (A) and Salbutamol sulphate microcrystals(B).

Figure 2 shows the DSC thermograms of Salbutamol sulphate pure and its microcrystals. The temperature of endotherm (T_m) of the microcrystal's all cases was almost the same in comparison with Salbutamol sulphate pure but it shows a slight reduction in T_m . On other hand microcrystal's also shows a significant reduction in enthalpy changes in comparison with Salbutamol sulphate pure. But both lowering of T_m and reduction of enthalpy was not concluded any type of incompatibility between drug and excipient. These changes attribute to the size reduction in microcrystals. Effect of stabilizers i.e HPMC on the crystal growth has been explained previously in several studies. The presence of dissolved impurities may affect the rate of crystallization, transition towards amorphous nature and even change crystal habit, because of their adsorption phenomenon on the nuclei and growing crystals. The adsorbed polymers stabilizes drug sterically and lowers surface energy and enthalpy of system.

However, the enthalpy of fusion, ΔH_f , as determined by differential scanning calorimetry, reduced much more which reflects a significant change in both the enthalpy and entropy of the Salbutamol sulphate crystals. Therefore it may conclude that the small amount of stabilizer was the cause of enthalpy reduction of the microcrystal's compared to pure Salbutamol sulphate.

3.1.3 Scanning Electron Microscopy

Figure 3. SEM photographs of various Salbutamol sulphate particles: (a) Pure drug; (b) Spray dried powder.



The morphology of pure Salbutamol sulphate shows non-homogeneous particles shapes and a broad particle size distribution was depicted in (Fig. 3a). In the in-situ-micronized technique gives drug powder which is recognizable uniform small particles which correlates with the particle size distribution of the dispersion (Fig. 3). The small particles with narrower particle size distribution resulted from the controlled crystallization phenomenon in the presence of stabilizer, which not only controls the particle size but also adsorb on the particles during the spray-drying process. Spherical particles with adsorbed stabilizer i.e HPMC prevents the presence of lots of agglomerates formed by crystal bridges between the flaky particles of the pure drug.

3.1.4 Fourier transform infrared (FT-IR) spectroscopy

The FTIR (Figure 4) of salbutamol sulphate has shown intense band at 1386.68 cm^{-1} , 1612.60 cm^{-1} , and 1386.68 cm^{-1} corresponding to the presence of functional groups such as Tri-methyl group, secondary amine group, and phenol group. The FTIR of **Spray dried powder** of salbutamol sulphate formulation has shown intense bands at 1388.41 cm^{-1} , 1610.35 cm^{-1} , and 1388.41 cm^{-1} which indicates no change in the functional groups such as Tri-methyl group,

secondary amine group, and phenol group and confirmed undisturbed structure of Salbutamol Sulphate. This indicated that there was no difference between the internal structures and conformation of these samples at the molecular level.

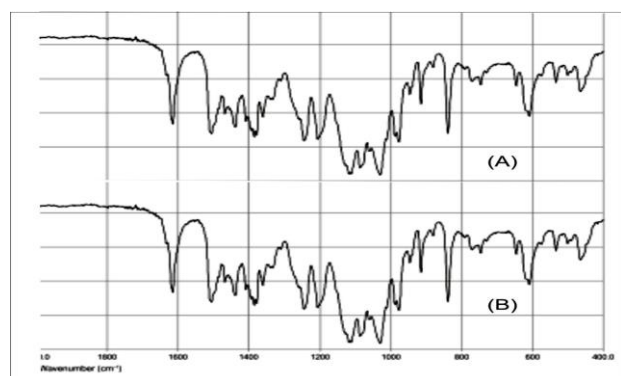


Figure 4. Fourier Transform Infrared Spectroscopy (FT-IR) of various Salbutamol sulphate particles: (a) Pure drug; (b) Spray dried powder.

3.2 Powder flow characterization

True density (D_{true}), bulk density (D_b), tap density (D_t), Carr's index (CI), angle of repose (α), and porosity for all formulations were calculated. All formulations showed identical D_{true} (1.44 ± 0.22 g/cm³) as comparison with pure drug (D_{true} (1.76 ± 0.57 g/cm³)) it shows lesser value for are attributed to its different crystalline nature. All formulations showed dissimilar D_b , D_t , CI, α and porosity. Direct linear proportionality ($r^2 = 0.958$) was found between CI and α showing good agreement between the two methods. Both CI and α data indicated good flow character of all formulations, which is needed to achieve satisfactory DPI formulation (Taylor et al., 2000). By comparing different formulations with pure drug powder, formulations showed the lowest D_b (0.61 ± 0.21 g/cm³), the lowest D_t (0.74 ± 0.88 g/cm³), and the highest porosity ($63.2 \pm 0.24\%$) whereas pure drug powder showed the highest D_b (0.94 ± 0.12 g/cm³), the highest D_t (0.98 ± 0.71 g/cm³), and the lowest porosity ($35.1 \pm 0.8\%$). This indicates that, contrary to pure drug powder, formulations have the lowest cohesiveness properties and lowest inter particulate forces. This could be attributed to spherical particle shape in case of formulations, which is likely to lead to increased void space between particles.

3.3 Response surface construction to optimize crystallization parameters

The mean particle size and Fine Particle Fraction (FPF) of Salbutamol sulphate obtained by using *in-situ* micronization technique with use of HPMC as a stabilizer was studied. There is also brief elaboration of effect of Antisolvent Addition Rate (ml/min), Stabilizer conc. (%) & Agitation rate (rpm) on crystal growth. For the optimization purpose we select Central Composite Design (Table 1 & 2) with linear and Quadratic as design model from mean particle size and Fine Particle Fraction (FPF) respectively for response surface category (Table 2). It gives 20 runs, with no blocks in the design. Three factors i.e. Antisolvent Addition Rate (ml/min), Stabilizer conc. (%) & Agitation rate (rpm) to be considered as independent variables. Response for mean particle size (Dependable Variable 1) and Fine Particle Fraction (FPF) (Dependable Variable 2) was analyzed with polynomial. Dependable Variable 1 ranges from 1.460 to 9.540 and for dependable Variable 2 it was from 43 to 78. Current design models do not required data transformation.

3.4 Mean Particle size

Correlation of addition rate was -0.016, stabilizer conc. was -0.663 and agitation rate was -0.425, with Mean Particle size (Dependable variable 1) shown in Figure. 5, Figure. 6 and Figure. 7 respectively. Addition rate, stabilizer conc., and agitation rate shows negative correlation. From this it was conclude that there was negative effect of addition rate, stabilizer conc., and agitation rate on the mean particle size.

3.5 Fine Particle Fraction (FPF)

Correlation of Addition rate was 0.285, Stabilizer concentration was 0.534 and agitation rate was 0.514 with fine particle fraction (Dependable variable 2) shown in Figure. 9, Figure. 10, and Figure. 11 respectively.

3.6 Optimization of process parameters

Commonly the high molecular weight hydrophilic molecules like Dextran, starch derivatives are not able to inhibit particle growth i.e crystallization process as that of cellulose ether with alkyl substitute e.g Hydroxy Propyl Methyl Cellulose (HPMC) and Methyl Cellulose (MC). This can be conclude that there should be interaction of polymers with newly formed surfaces can only resulted into inhibition of crystal growth.

Table 1. Experimental runs according to Central composite design with their coded values.

Standard	Runs	A: Addition rate	B: Stabilizer conc.	C:Agitation rate	Mean Particle Size	Fine Particle Fraction (FPF)
2	1	1.00	-1.00	-1.00	7.85	48
7	2	-1.00	1.00	1.00	2.65	69
8	3	1.00	1.00	1.00	1.46	78
16	4	0.00	0.00	0.00	5.21	64
4	5	1.00	1.00	-1.00	6.34	52
17	6	0.00	0.00	0.00	5.21	64
11	7	0.00	-1.68	0.00	6.32	51
1	8	-1.00	-1.00	-1.00	9.54	43
19	9	0.00	0.00	0.00	5.21	64
6	10	1.00	-1.00	1.00	3.98	69
20	11	0.00	0.00	0.00	5.21	64
10	12	1.68	0.00	0.00	5.71	59
15	13	0.00	0.00	0.00	5.21	64
14	14	0.00	0.00	1.68	4.21	73
3	15	-1.00	1.00	-1.00	3.52	54
5	16	-1.00	-1.00	1.00	5.98	43
18	17	0.00	0.00	0.00	5.21	64
13	18	0.00	0.00	-1.68	3.76	62
12	19	0.00	1.68	0.00	2.76	71
9	20	-1.68	0.00	0.00	4.76	55

Table 2. Design Summary for 30 runs with quadratic and 2FI as design models.

Factor	Name	Units	Type	Low Actual	High Actual	Low Coded	High Coded	Mean	Std. Dev.
A	Adition rate	ml/min	Numeric	-1.00	1.00	-1.000	1.000	0.000	0.826
B	Stabilizer conc.	%	Numeric	-1.00	1.00	-1.000	1.000	0.000	0.826
C	Agitation rate	rpm	Numeric	-1.00	1.00	-1.000	1.000	0.000	0.826

Resp- onse	Name	Analysis	Min.	Max.	Mean	Std. Dev.	Ratio	Trans	Model
Y1	Mean Particle Size	Polynomial	1.460	9.540	5.005	1.76	6.534	None	Linear
Y2	Fine Particle Fraction (FPF)	Polynomial	43.00	78.00	60.55	9.48	1.814	None	Quadratic

Design-Expert® Software

Correlation: -0.016

Color points by

Run

20

1

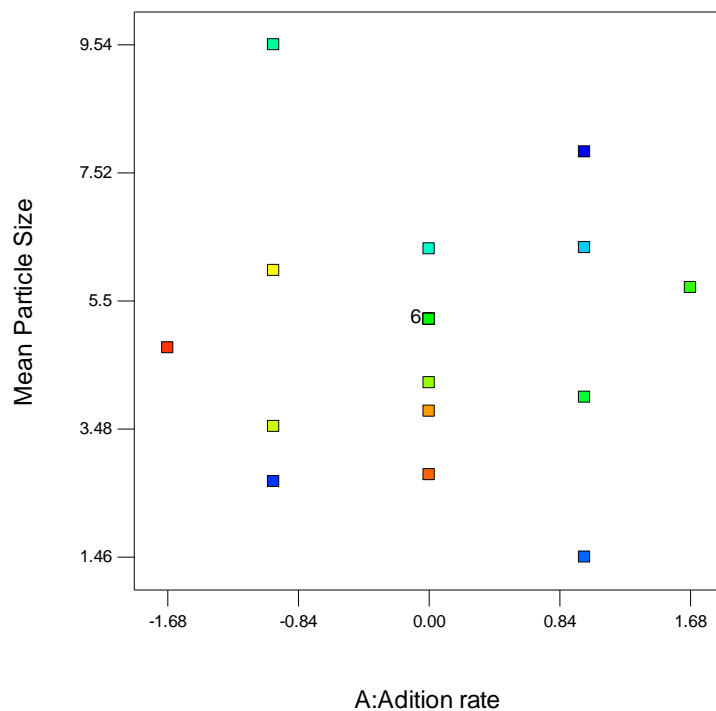


Figure 5. Graph showing correlation between Addition rate and Mean particle size.

Design-Expert® Software

Correlation: -0.663

Color points by

Run

20

1

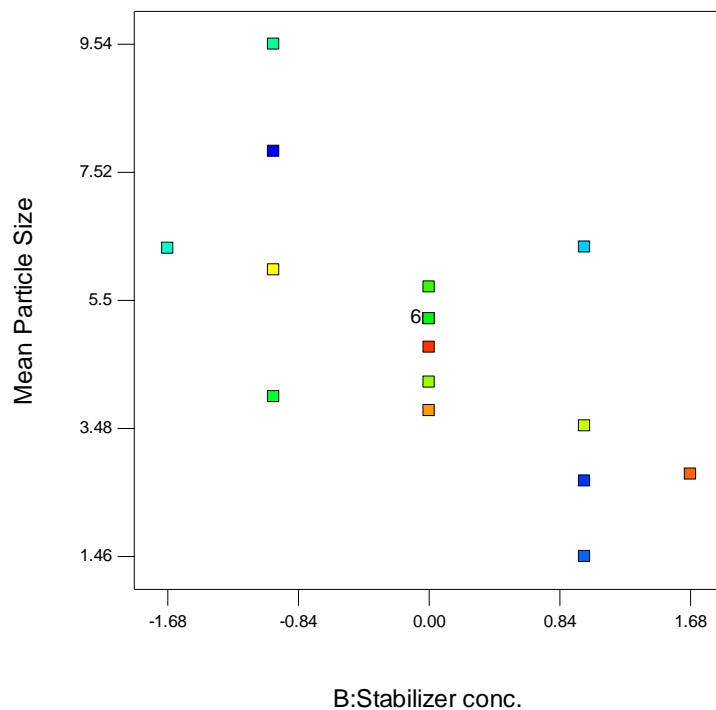


Figure 6. Graphs showing correlation between Stabilizer conc. and Mean particle size

Design-Expert® Software

Correlation: -0.425

Color points by

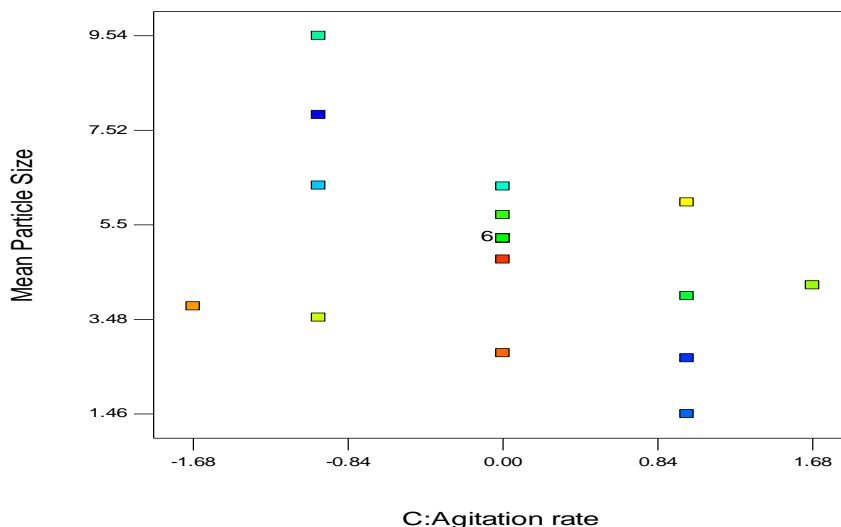


Figure 7. Graphs showing correlation between Agitation rate and Mean particle size

The cubic and quadratic model was aliased. This means not enough experiments have been run to independently estimate all the terms for this model. The suggested model is Linear (Table 3 and 4).

Table 3. Sequential Model Sum of Squares [Type I] for mean particle size.

Source	Sum of Squares	df	Mean Square	F Value	p-value Prob > F	
Mean vs Total	501.00	1	501.00			
<u>Linear vs Mean</u>	<u>38.78</u>	<u>3</u>	<u>12.93</u>	<u>8.71</u>	<u>0.0012</u>	<u>Suggested</u>
2FI vs Linear	6.22	3	2.07	1.54	0.2513	
Quadratic vs 2FI	1.86	3	0.62	0.40	0.7582	
Cubic vs Quadratic	14.44	4	3.61	17.87	0.0018	Aliased
Residual	1.21	6	0.20			
Total	563.52	20	28.18			

Table 4. Model Summary Statistics for mean particle size.

Source	Std. Dev.	R-Squared	Adjusted R-Squared	Predicted R-Squared	PRESS	
<u>Linear</u>	<u>1.22</u>	<u>0.6203</u>	<u>0.5491</u>	<u>0.3013</u>	<u>43.68</u>	<u>Suggested</u>
2FI	1.16	0.7198	0.5905	-0.2072	75.48	
Quadratic	1.25	0.7496	0.5243	-0.9441	121.55	
Cubic	0.45	0.9806	0.9386	-3.2747	267.27	Aliased

ANOVA (Table 5) suggested for the design is as follows. The Model F-value of 8.71 implies the model is significant. There is only a 0.12% chance that a "Model F-Value" this large could occur due to noise. Values of "Prob> F" less than 0.0500 indicate model terms are significant. In this case B, C are significant model terms.

Table 5. ANOVA for Response Surface Quadratic Model Analysis of variance table [Partial sum of squares - Type III] for mean particle size.

Source	Sum of		Mean	F	p-value	
	Squares	df	Square	Value	Prob> F	
Model	38.78	3	12.93	8.71	0.0012	significant
A-Adition rate	0.016	1	0.016	0.011	0.9195	
B-Stabilizer conc.	27.47	1	27.47	18.51	0.0005	
C-Agitation rate	11.30	1	11.30	7.62	0.0140	
Residual	23.74	16	1.48			
Lack of Fit	23.74	11	2.16			
Pure Error	0.000	5	0.000			
Cor Total	62.52	19				

Final Equation in Terms of Coded Factors:

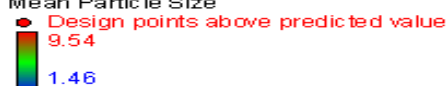
$$\begin{aligned} \text{Mean Particle Size} &= \\ &+5.00 \\ &-0.034 * A \\ &-1.42 * B \\ &-0.91 * C \dots\dots\dots(4) \end{aligned}$$

Final Equation in Terms of Actual Factors:

$$\begin{aligned} \text{Mean Particle Size} &= \\ &+5.00500 \\ &-0.033851 * \text{Adition rate} \\ &-1.41813 * \text{Stabilizer conc.} \\ &-0.90967 * \text{Agitation rate} \dots\dots\dots(5) \end{aligned}$$

Design-Expert® Software

Mean Particle Size



X1 = A: Adition rate
X2 = B: Stabilizer conc.

Actual Factor
C: Agitation rate = 0.00

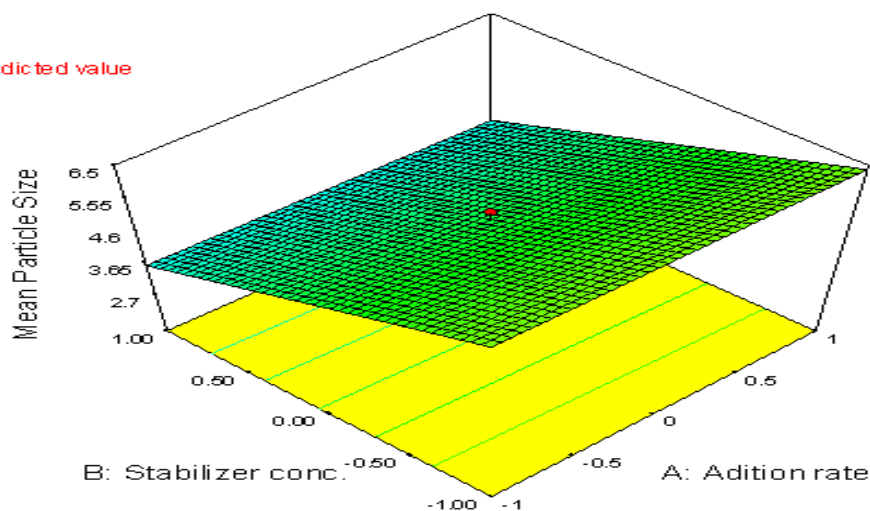


Figure 8. Response surface graph for Mean particle size with respect to Stabilizer conc. and Addition rate as prominent factors.

Design-Expert® Software

Correlation: 0.285

Color points by

Run

20

1

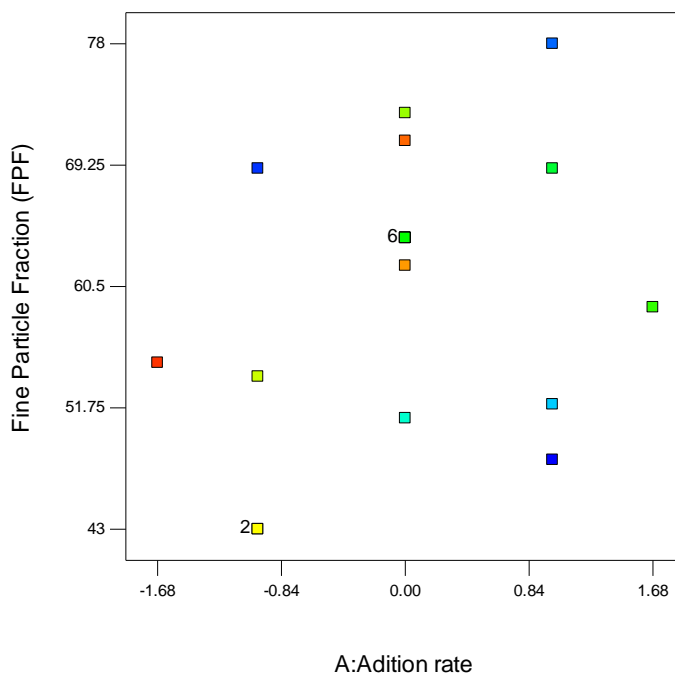


Figure 9 Graphs showing correlation between Addition rate and fine particle fraction.

Design-Expert® Software

Correlation: 0.534

Color points by

Run

20

1

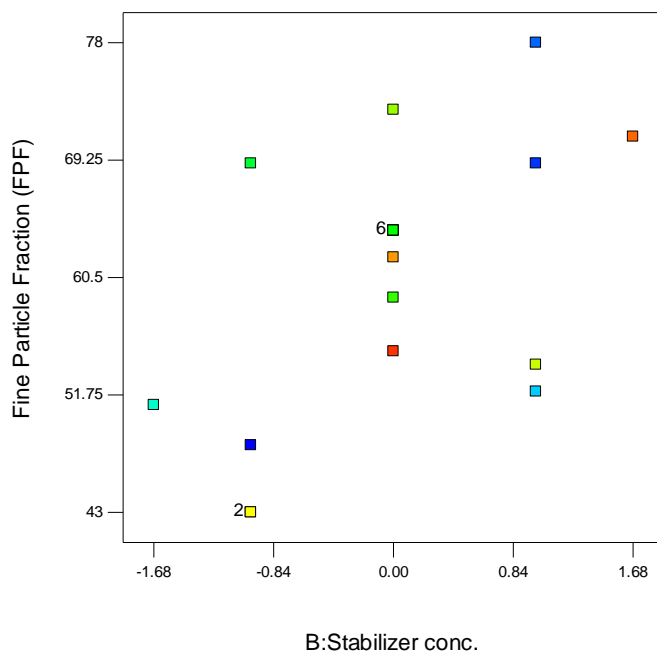


Figure 10. Graphs showing correlation between Tween 20 and standard deviation of mean particle size

Design-Expert® Software

Correlation: 0.514

Color points by

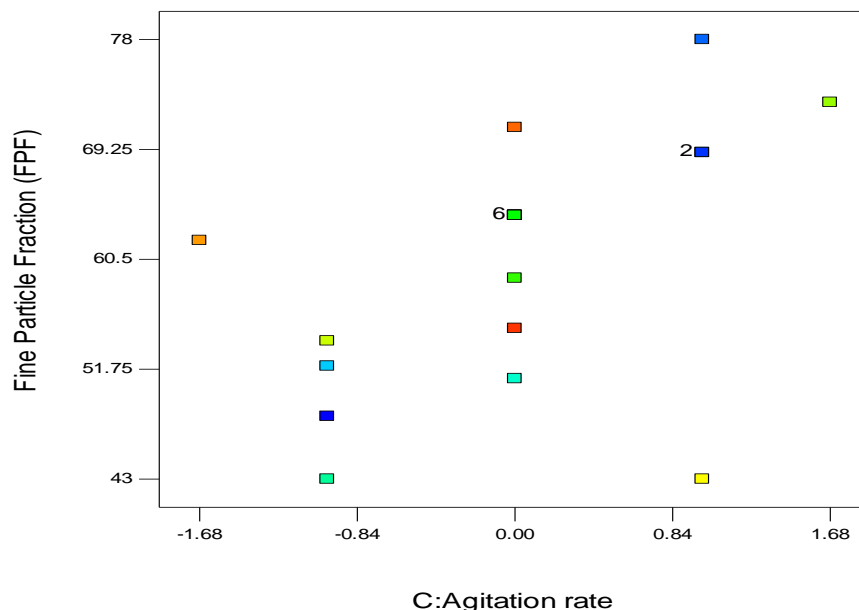


Figure 11. Graphs showing correlation between Addition rate and standard deviation of mean particle size

The cubic model is aliased. This means not enough experiments have been run independently estimate all the terms for this model. The suggested model is Quadratic (Table 6 and 7).

Table 6. Sequential Model Sum of Squares [Type I] for Standard Deviation of mean particle size.

Source	Sum of Squares	df	Mean Square	F Value	p-value	Prob> F
Mean vs Total	73326.05	1	73326.05			
Linear vs Mean	1133.18	3	377.73	9.08	0.0010	Suggested
2FI vs Linear	250.00	3	83.33	2.61	0.0962	
Quadratic vs 2FI	223.84	3	74.61	3.89	0.0445	Suggested
Cubic vs Quadratic	121.32	4	30.33	2.58	0.1442	Aliased
Residual	70.61	6	11.77			
Total	75125.00	20	73756.25			

Table 7. Model Summary Statistics for Standard Deviation of mean particle size

Source	Std. Dev.	R-Squared	Adjusted R-Squared	Predicted R-Squared	PRESS
Linear	6.45	0.6299	0.5605	0.3431	1181.75
2FI	5.66	0.7689	0.6622	0.0713	1670.60
Quadratic	4.38	0.8933	0.7973	0.1805	1474.16
Cubic	3.43	0.9608	0.8757	-7.6518	15564.15

ANOVA (Table 8) suggested for the design is as follows. The Model F-value of 9.30 implies the model is significant. There is only a 0.09% chance that a "Model F-Value" this large could occur due to noise. Values of "Prob> F" less than 0.0500 indicate model terms are significant. In this case A, B, C, AC, A2 are significant model terms.

Table 8 ANOVA for Response Surface 2FI Model Analysis of variance table [Partial sum of squares - Type III] for Standard Deviation of mean particle size.

Source	Sum of Squares	df	Mean Square	F Value	p-value Prob > F	
Model	1607.02	9	178.56	9.30	0.0009	significant
A-Adition rate	146.48	1	146.48	7.63	0.0200	
B-Stabilizer conc.	512.19	1	512.19	26.69	0.0004	
C-Agitation rate	474.50	1	474.50	24.72	0.0006	
AB	72.00	1	72.00	3.75	0.0815	
AC	128.00	1	128.00	6.67	0.0273	
BC	50.00	1	50.00	2.61	0.1376	
A ²	173.23	1	173.23	9.03	0.0132	
B ²	60.73	1	60.73	3.16	0.1056	
C ²	0.87	1	0.87	0.045	0.8360	
Residual	191.93	10	19.19			
Lack of Fit	191.93	5	38.39			
Pure Error	0.000	5	0.000			
Cor Total	1798.95	19				

Final Equation in Terms of Coded Factors:

$$\begin{aligned} \text{Fine Particle Fraction (FPF)} &= \\ &+64.15 \\ &+3.28 * A \\ &+6.12 * B \\ &+5.89 * C \\ &-3.00 * A * B \\ &+4.00 * A * C \\ &+2.50 * B * C \\ &-3.47 * A^2 \\ &-2.05 * B^2 \\ &+0.25 * C^2 \dots\dots\dots(6) \end{aligned}$$

Final Equation in Terms of Actual Factors:

$$\begin{aligned} \text{Fine Particle Fraction (FPF)} &= \\ &+64.15182 \\ &+3.27507 * \text{Adition rate} \\ &+6.12409 * \text{Stabilizer conc.} \\ &+5.89446 * \text{Agitation rate} \\ &-3.00000 * \text{Adition rate} * \text{Stabilizer conc.} \\ &+4.00000 * \text{Adition rate} * \text{Agitation rate} \\ &+2.50000 * \text{Stabilizer conc.} * \text{Agitation rate} \\ &-3.46709 * \text{Adition rate}^2 \\ &-2.05287 * \text{Stabilizer conc.}^2 \\ &+0.24522 * \text{Agitation rate}^2 \dots\dots\dots(7) \end{aligned}$$

Design-Expert® Software

Fine Particle Fraction (FPF)

○ Design points below predicted value



X1 = A: Addition rate

X2 = B: Stabilizer conc.

Actual Factor

C: Agitation rate = 0.00

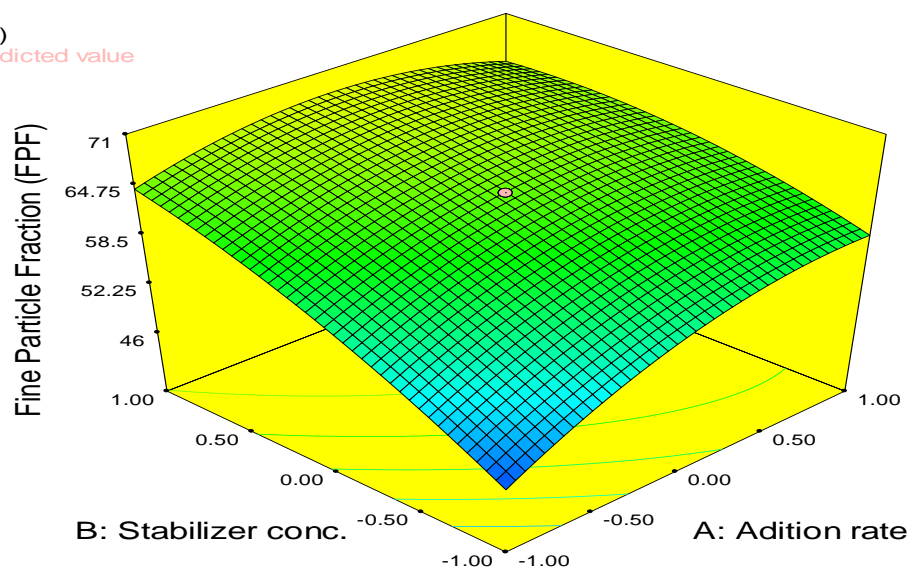


Figure 12. Response surface graph for Standard deviation of Mean particle size with respect to Cremophor EL and Tween 20 conc. As a prominent factors.

The fine particle fraction of spray dried Salbutamol Sulphate crystals was shown in Figure 12. The fine particle fraction was the largest where there is high amount of stabilizer concentration and high addition rate up to particular extent. Statistical analysis of the Fine Particle Fraction (FPF) produced by different formulations by a two-way ANOVA test showed that the concentration of the stabilizer and addition rate had a significant effect on the particle size of the microcrystal's while the agitation rate did not have a significant effect on the particle size.

Micron-sized Salbutamol sulphate was prepared by a *in-situ* precipitation and stabilization of the micronized drug particles by the use of hydroxyl propylmethylcellulose (HPMC). HPMC adsorbed on newly formed surfaces and prevents crystal growth by steric hindrances which can also resulted into lowering of surface energy and enthalpy of system. Sterically stabilization of newly formed crystals by adsorbed HPMC molecules concludes particle size range in inhalation range.

In formulation optimization, Fine Particle Fraction (FPF) was the critical parameter to observed and require control. Fine fraction depends on amount of HPMC available to adsorb on newly formed particles and different processing parameters. During crystallization process particles are formed actual and in spray drying process it can be agglomerates to form

fraction of large particles. These large particles are the product of agglomeration of non HPMC adsorbed drug particles. We select Fine Particle Fraction (FPF) as the dependable variable in our study. Fine Particle Fraction (FPF) variable majorly depends on the amount of stabilizer to be added. High concentration of HPMC makes sufficient availability of HPMC to get absorb on newly formed particles and further increase in the Fine Particle Fraction (FPF) results. So concentration of HPMC was affecting the Fine Particle Fraction (FPF) and to be optimized further. The adsorbed HPMC also improves micromeritic properties of drug crystals.

However, in comparison of non-ionic surfactant as stabilizers cellulose derivatives are having more acceptances because of their biocompatibility, biodegradability and cost effectively.

For the crystal growth, saturation was the first step leads to supersaturation. Supersaturation state further leads to generation of small crystals and it further consumed by nucleation stage. After nucleation state further crystal growth is there. Crystal size and distribution depends on the rate of supersaturation and thereby nucleation. Thus the addition rate of antisolvent further improves the mean particle size and their Fine Particle Fraction (FPF) as shown in the equation 4, 5, 6 and 7. Higher addition rate of antisolvent decreases

the mean particle size by increased rate of supersaturation and thereby nucleation. The smaller particles produced by high addition rate also stabilized by the stabilizer added i.e. HPMC.

The final Particle Size Distribution in a precipitation process is determined by the relative balance of the kinetic rates of nucleation and crystal growth. The Particle Size Distribution, however, is dependent on the initial number of nuclei formed and also on the growth rate of those nuclei.

Thus supersaturation can be consumed by crystal growth leading to higher particle sizes. As the antisolvent addition rate is increased, a shift in the balance of micro- to mesomixing occurs. Mesomixing leads to localization of high levels of supersaturation in turbulent eddies and concomitant high rates of nucleation. Thus large numbers of primary nuclei are formed which possess a large surface area, and undergo limited growth in regions of lower local supersaturation leading to a narrow particle size distribution.

Agitation rate improves micromixing but lowers local supersaturation by facilitating turbulent mesomixing and thereby crystal growth was a resultant effect and the mean particle size to be increased as shown in the equation 4, 5, 6 and 7. Crystal growth involves an element of volume-diffusion control where solute molecules must diffuse through a diffusion barrier around nascent crystals. Increasing the stirring speed facilitates diffusion by decreasing the thickness of the stagnant boundary layer, hence affecting the balance between nucleation and crystal growth. Both of these reasons stirring speed broaden particle size distribution.

We set constrains for the Independent variables (Table .9). In order to achieve of targeted response i.e. minimum mean particle size and their Fine Particle Fraction (FPF), the 33 solutions suggested by the Design Expert software with descending order of desirability. Form the 33 solutions first 10 solutions with high desirability were sown in Table 10.

Table 9 Constraints for the variables

Name	Goal	Lower Limit	Upper Limit	Lower Weight	Upper Weight	Importance
Addition rate	is in range	-1	1	1	1	3
Stabilizer conc.	is in range	-1	1	1	1	3
Agitation rate	is in range	-1	1	1	1	3
Mean Particle Size	is in range	1	5	1	1	3
Fine Particle Fraction (FPF)	maximize	43	78	1	1	3

Table 10 Formulations (up to 10) according to the descending order of desirability.

Number	Addition rate	Stabilizer conc.	Agitation rate	Mean Particle Size	Fine Particle Fraction (FPF)	Desirability
F1	0.72	1.00	0.99	2.66742	78.0176	1.000
F2	0.74	0.97	1.00	2.69653	78.0072	1.000
F3	0.48	0.98	1.00	2.68907	78.017	1.000
F4	0.61	0.98	0.99	2.69526	78.0509	1.000
F5	0.68	0.97	0.99	2.69984	78.0041	1.000
F6	0.51	0.99	0.99	2.67802	78.0052	1.000
F7	0.65	0.96	1.00	2.70627	78.0748	1.000
F8	0.66	0.98	0.99	2.69397	78.026	1.000
F9	0.53	0.98	1.00	2.6866	78.0546	1.000
F10	0.51	0.98	0.99	2.68799	78.0216	1.000

From solutions the solution with highest desirability we selected as optimized formulation i.e. F1 formulation.

3.7 Evaluation of optimized formulation for their aerodynamic properties.

Optimised formulation F1 had evaluated by the deposition pattern by MSLI. The results indicated that the Salbutamol Sulphate particles of high fine fraction and spherical morphology had shown significantly better aerosol performance. Optimized product corresponding to a decrease in stage 1 deposition along with a subsequent increase in stages 3 and 4 in the MSLI. It is worth that the particles were uniform in the presence of HPMC showed the highest FPF loaded and FPF emitted of 78 (1%) and 84 (3%) respectively, depositing mainly on stages 3 and 4, with much lower amounts collected on the higher stages of the MSLI.

According to definition of D_{ae}

$$D_{ae} = D_{eq} \sqrt{\frac{\rho_p}{\rho_0 \chi}} \quad (8)$$

$$D_{eq} = 3 \sqrt{\frac{6V}{\pi}} \quad (9)$$

Where D_{eq} is the volume-equivalent diameter of the particle, V is the particle volume, ρ_p is the particle bulk density, ρ_0 is the unit density, and χ is the dynamic shape factor, defined as the ratio of the drag force on a particle to the drag force on the particle volume-equivalent sphere at the same velocity. Thus, D_{ae} can be reduced by one or more of the following manipulations : (1) decreasing the volume-equivalent particle diameter (D_{eq}), (2) reducing the particle density (ρ_p), and (3) increasing the particle dynamic shape factor (χ). Optimized budesonide particles had the thin thickness, and the spherical particles were calculated to be of higher D_{eq} . The agglomerates formed by the spherical particles had a smooth surface, which effectively increased the interagglomerate distance and lowered the van der Waals attractive force. Furthermore, the surface asperities may also reduce the effective area of contact between agglomerates. Namely, the agglomerates had a lower bulk density. Third, the χ value for the particles of spherical shapes could be smaller. On account of the above reasons, the D_{ae} of these spherical particles was intermediate so that they had high FPF values.

4. Conclusion

HPMC was acts as biocompatibility, biodegradability and cost effectively and has been shown to be eminently suitable stabilizer in *In-situ* Microcronication technique for Salbutamol Sulphate. Physical Stability of micronized spray dried product was confirmed by XRD, FTIR, DSC and SEM. The PSD was shown to depend on the hydrodynamic conditions provided by the HPMC which acts as stabilizers. Sstabilizers played important roles in the formation and growth of Salbutamol Sulphate particles. In this study the factors i.e. stirrer speeds investigated were 500(-1), 1000(0) and 1500 (1) rpm, addition rate of non-solvent i.e ethanol was studied at 50(-1), 100(0) and 150(1) g /min and stabilizer conc. were 0.5(-1), 1(0) and 1.5 %(1) controlling the microcrystallization of Salbutamol Sulphate by *In-situ* Microcronication technique have been identified. Optimized formulation was identified and characterized to determine their suitability for pulmonary delivery by using MSLI. Higher FPF values were performed by the agglomerates formed by spherical particles had intermediate volume-equivalent particle diameter with less standard deviation, lower bulk density, low porosity and larger dynamic shape factor. The antisolvent precipitation due to its being simple and cost effective will be a prosperous pathway for DPI application.

REFERENCES

1. Sakagami, M., 2006. In vivo, in vitro and ex vivo models to assess pulmonary absorption and disposition of inhaled therapeutics for systemic delivery. *Adv. Drug Deliv. Rev.* 58, 1030–1060.
2. Newman, S., Wilding, I.R., Hirst, P.H., 2010. Human lung deposition data: the bridge between in vitro and clinical evaluations for inhaled drug products? *Int. J. Pharm.* 208, 49–60.
3. Misra, A., Hickey, A.J., Rossi, C., Borchard, G., Terada, H., Makino, K., Fourie, P.B., Colombh, P., 2011. Inhaled drug therapy for treatment of tuberculosis. *Tuberculosis* 91, 71–81.
4. Sherwood, L., 2010. *Human Physiology: From Cells to Systems*, 7th ed. Brooks/Cole Cengage Learning, United States of America.
5. Sung, J.C., Pulliam, B.L., Edwards, D.A., 2007. Nanoparticles for drug delivery to the lungs. *Trends Biotechnol.* 25, 563–570.
6. Bhavna, Ahmed, F.J., Mittal, G., Jain, G.K., Malhotra, G., Khar, R.K., Bhatnagar, A., 2009.
7. Nano-salbutamol dry powder inhalation: a new approach for treating bronchoconstrictive

- conditions. *Eur. J. Pharmaceut. Biopharmaceut.* 71, 282–291.
8. Cook, R.O., Pannu, R.K., Kellaway, I.W., 2005. Novel sustained release microspheres for pulmonary drug delivery. *J. Control. Release* 104, 79–90.
 9. Learoyd, T.P., Burrows, J.L., French, E., Seville, P.C., 2008. Modified release of beclomethasonedipropionate from chitosan-based spray-dried respirable powders. *Powder Technol.* 187, 231–238.
 10. Learoyd, T.P., Burrows, J.L., French, E., Seville, P.C., 2009. Sustained delivery by leucine-modified United States of America chitosan spray-dried respirable powders. *Int. J. Pharmaceut.* 372, 97–104.
 11. Kwon, M.J., Bae, J.H., Kim, J.J., Na, K., Lee, E.S., 2007. Long acting porous microparticle for pulmonary protein delivery. *Int. J. Pharmaceut.* 333, 5–9.
 12. National Heart, Lung and Blood Institute, National Institute of Health—Global Initiative for Asthma: Global Strategy for Asthma Management and Prevention. NHBLI/WHO workshop report, 1995, NIH publication number 95-3659.
 13. Zanen, P., Lammers, J-W.J., 1995. Sample sizes for comparative inhaled corticosteroid trials with emphasis on showing therapeutic equivalence. *J. Clin. Pharmacol.* 48, 179–184.
 14. Pasquali, R. Bettini, F. Giordano, Solid-state and particle engineering with supercritical fluids in pharmaceuticals, *European J. Pharmaceutical Sciences* 27 (2006) 299–310.
 15. V. Naini, P.R. Byron, E.M. Phillips, Physicochemical stability of crystalline sugar and their spray-dried forms: dependence upon relative humidity and suitability for use in powder inhalers, *Drug Development and Industrial Pharmacy* 24 (1998) 895–909.
 16. Malcolmson, R.J., Embleton, J.K., 1998. Dry powder formulations for pulmonary delivery. *Pharm. Sci. Technol. Today* 1, 394–398.
 17. Müller, R.H., Peters, K., Becker, R., Kruss, B., 1996. Nanosuspensions for the i.v. administration of poorly soluble drugs—stability during sterilization and long-term storage. *Proc. Int. Symp. Control Rel. Bioact. Mater.* 22, 574–575.
 18. Roberts, R.J., Rowe, R.C., York, P., 1994. The relationship between indentation hardness of organic solids and their molecular structure. *J. Mater. Sci.* 29, 2289–2296.
 19. Parrott, E.L., 1990. Comminution. In: Swarbrick, J., Boylan, J.C. (Eds.), *Encyclopedia of Pharmaceutical Technology*, vol. 3. Marcel Decker, New York, pp. 101–121.
 20. Ogura, K., Sobue, H., 1970. Changes in morphology with milling of the commercial microcrystalline cellulose. *J. Appl. Polymer Sci.* 14, 1390–1393.
 21. Ward G.H., Schultz, R.K., 1995. Process-induced crystallinity changes in albuterol sulfate and its effect on powder physical stability. *Pharm. Res.* 12, 773–779.
 22. Schott, H., 1985. Colloidal dispersions. In: *Remington's Pharmaceutical Sciences. The Philadelphia College of Pharmacy and Science, Philadelphia*, pp. 286–289.
 23. Buckton, G., 1997. Characterization of small changes in the physical properties of powders of significance for dry powder inhaler formulations. *Adv. Drug Del. Rev.* 26, 17–27.
 24. Williams, R.O., Brown, J., Liu, J., 1999. Influence of micronization method on the performance of a suspension triamcinolone acetonide pressurized metered-dose inhaler formulation. *Pharm. Dev. Technol.* 4, 167–179.
 25. Feeley, J.C., York, P., Sumbly, B.S., Dicks, H., 1998. Determination of surface properties and flow characteristics of salbutamol sulphate, before and after micronization. *Int. J. Pharm.* 172, 89–96.
 26. Mackin, L., Sartnurak, S., Thomas, I., Moore, S., 2002. The impact of low levels of amorphous material (<5%) on the blending characteristics of a direct compression formulation. *Int. J. Pharm.* 231, 213–226.
 27. Taylor, K.M.G., Pancholi, K., Wong, D.Y.T., 1999. In-vitro evaluation of dry powder inhaler formulations of micronized and milled nedocromil sodium. *Pharm. Pharmacol. Commun.* 5, 255–257.
 28. G.M.J. Schmidt, Topochemistry. Part III. The crystal chemistry of some trans-cinnamic acids, *J. Chem. Soc.* (1964) 2014.
 29. HartwigSteckel, Norbert Rasenack, Bernd W. Müller, In-situ-micronization of disodium cromoglycate for pulmonary delivery, *European Journal of Pharmaceutics and Biopharmaceutics* 55 (2003) 173–180
 30. HartwigSteckel a, Norbert Rasenack a, Peter Villax b, Bernd W. Müller a, In vitro characterization of jet-milled and in-situ-micronized fluticasone-17-propionate, *International Journal of Pharmaceutics* 258 (2003) 65–75